Pas très clair pour moi.
L'important de mon point de vue est de dire que le fait d'utiliser la position supine pour "recaler" par optimisation les paramètres mécaniques et pour "évaluer" le modèle biaise d'une certaine manière l'évaluation et sans doute sous-estime les limites du modèle. D'où l'intérêt d'une évaluation sur une 3e position.

A new biomechanical breast model

3.1 Introduction

A State of the art in breast finite elements modeling was ~~described~~ provided previously. Three models were identified representing the cutting-edge technologies in the field. These models use prone MRI to create the breast reference geometry and supine MRI to ~~compute~~ estimate patient-specific tissues mechanical properties. The models were evaluated using the measured and the estimated positions of ~~the~~ superficial fiducial landmarks or internal anatomical landmarks in the supine configuration. However, the authors assumed different boundary conditions and considered different tissues types. In addition, none of the previous works have quantitatively evaluated the proposed model on an additional data set of the same patient.

This chapter ~~present~~ introduces a new biomechanical model developed by combining the best practices and concepts proved by previous works. To be as realistic as possible, our model considered breast heterogeneity, anisotropy, sliding boundary conditions, initial pre-stresses and personalized hyper-elastic properties of breast tissue. In addition, new types of soft tissue were included representing the breast support matrix composed of suspensory ligaments and fascias. Moreover, our model was built using prone and supine breast configurations and was evaluated in supine tilted configuration (≈45 deg) of the same volunteer.

In the first part of this chapter the data acquisition protocol is described and details on numerical methods and softwares used to extract the patient-specific breast geometry are given. Next, the different components of the finite elements mesh are presented and the mesh quality is assessed using shape parameters. Then, the assumptions on boundary conditions and materials models are explained. Finally, the model optimization process is detailed and results on patient-specific parameters and breast reference configuration are presented.

On ne prend pas en compte l'anisotropie des tissus mais une anisotropie "indirecte" liée à la présence des ligaments, non ?

3.2 Geometry extraction

Geometry extraction is the first step in FE analysis, and it consists of obtaining the 3D surfaces of the breast. We use the MR images to obtain the patient-specific breast volumes and the surrounding soft tissues distribution. Prior to surface extraction, the MRI volume is segmented and mapped to a single reference system. The next section describes the imaging acquisition protocol and the numerical method used to generate the 3D patient-specific breast geometry.

3.2.1 Data acquisition

The images were acquired with a Siemens 3T scanner with T2 weighted image sequences. The in-plane image resolution was 0.5x0.5 mm, and the slice thickness was 0.6 mm. During this acquisition, the contact between the breasts and the contours of the MRI tube, or with the patient body (arms, thorax), was minimized.

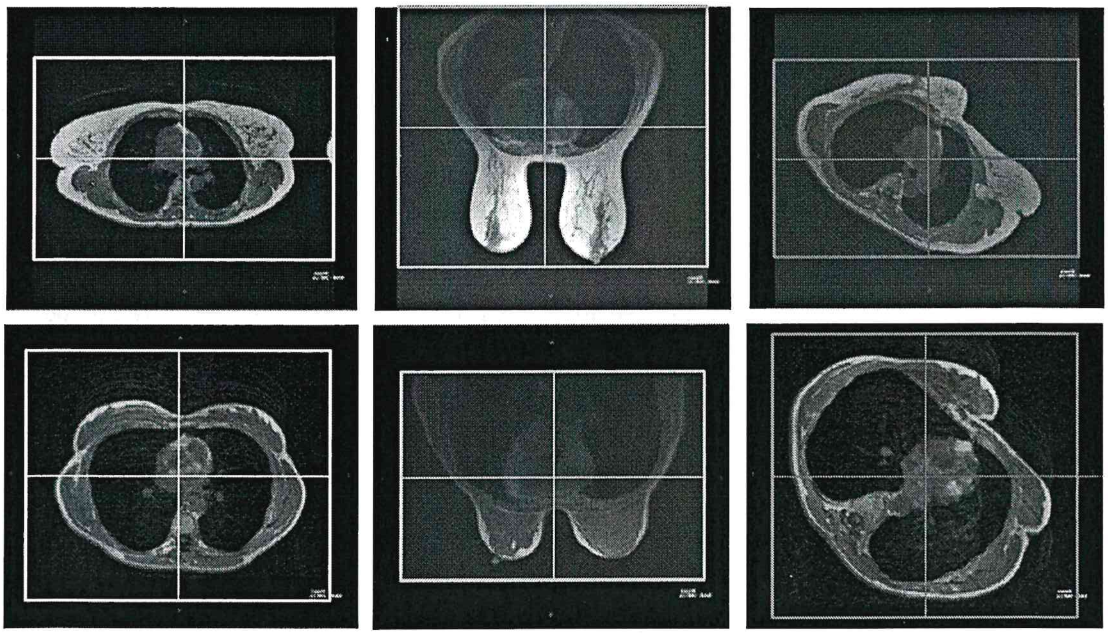

Figure 3.1: MRI images in three breast configuration: first line- subject 1; second line- subject 2

~~The~~ Two volunteers t~~aking part to this study~~ agreed to participate in ~~an experiment part of~~ a pilot study approved by an ethical committee (MammoBio MAP-VS pilot study). The volunteers are 59 and 58 years old and have A-cup (subject 1) and F-cup (subject 2) breast size respectively.

Three different positioning configurations are considered: prone, supine and supine titled (45 deg). The positions were chosen to assess the largest possible deformations with minimal contact areas between the volunteer and the relatively narrow MRI scanner tunnel.

que veux-tu dire par "internal organs" ?

Il faut choisir entre l'emploi du présent ou du passé dans la description du protocole

3.2.2 Image segmentation

A semi-automated active contour method proposed by ITK-Snap software is used to segment the pectoral muscle, the breast and the internal organs from MR images.

The segmentation process for one tissue type is performed progressively by small regions of interest (ROI, see Figure 3.2.a). For each ROI the segmentation of one tissue takes place in 3 steps (Figure 3.2):

une référence biblio ?

1. Firstly, the random forest algorithm is used to compute the probability of a pixel to belong or not to the segmented tissue. The training data set is manually selected by the user and includes state and space characteristics such as voxel grey intensity, voxel's neighbors intensity (with variable radius of neighboring), and (x; y; z) voxel position (Figure 3.2.c).

2. Secondly, spherical seeds point with variable radius are placed on the new synthetic volume to mark the connected ~~components bellowing~~ to the segmented tissue (Figure 3.2.d). c'est la première fois que tu parles de ce "synthetic volume". Il faudrait l'expliquer en l'introduisant dans le point 1. ci-dessus.

3. Finally, the placed seed point will evolve in the 3D space with a speed and direction derived from the pixel intensity and sign in the synthetic volume (Figure 3.2.d).

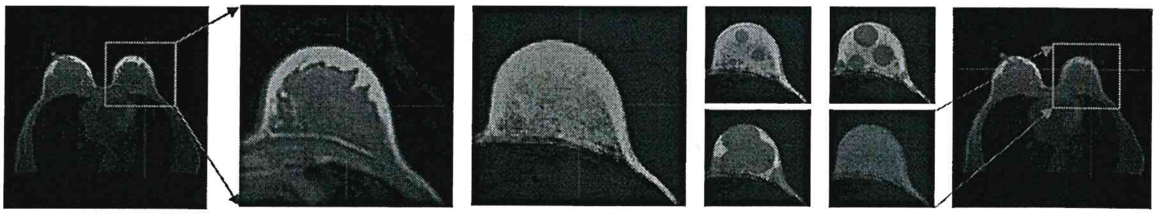

a) MR image (3D) b) ROI selection c) Synthetic volume d) Region growing (3D) e) Segmented fatty tissues (3D): right breast.

Figure 3.2: Breast tissues segmentation on the breast MRI of the second ~~subject~~ volunteer. Prone breast configuration. White-voxel belongs to breast tissue; blue - voxel don't belongs to fatty tissue

Il n'y a que des voxels "gris" je ne comprends pas...

After segmentation, an additional manual correction was performed to refine components boundaries. Simple erosion and dilatation operations were applied on breast and muscle segmented volumes in order to obtain smoother connected components. Then, to avoid tissues overlapping at muscle-breast juncture, ~~border~~ binary operations were used.

The process was repeated for both volunteers and for each breast configuration: supine, prone and supine tilted.

quel est l'intérêt de le faire dans ces deux configurations puisque le modèle n'est défini que dans la position prone ?

are indeed

3.2.3 Image registration

During the imaging acquisition process, the subject is moved in and out side the MRI scanner. Therefore, the breast not only undergoes an elastic transformation, but also a rigid one. Prior to image acquisition, four landmarks are fixed on the chest wall. The landmarks are placed on sternum and inframammary fold lines; these regions known to be rich in fibrous ligaments limiting the soft tissues' elastic deformation. To assess the body position changes between the two configurations a rigid transform is computed by minimizing the Euclidian distance of the four points defined by the four landmarks. The transformation is estimated using the iterative closest point (ICP) algorithm proposed by ITK library.

However, because of ~~breast hyperelasticity~~, the computed rigid transformation is not accurate enough. Therefore, a second registration step is performed by aligning the bone structures of the anterior part of thoracic cage from prone and supine tilted positions to the supine one. The muscular tissues mask previously segmented are used in order to remove body soft tissues. The image registration is implemented using the ~~descendant~~ descent gradient based algorithm minimizing the images cross correlation (ITK library).

Figure 3.3 shows overlapping prone-supine and supine tilted-supine breast images in the transversal plane after registration. The anterior part of the chest line is wall e aligned, however there are some differences because of elastic thoracic cage deformations due to hand positions or body-mass force reparation.

que veux-tu dire ?

the small local deformations of skin soft tissues in the chest wall region

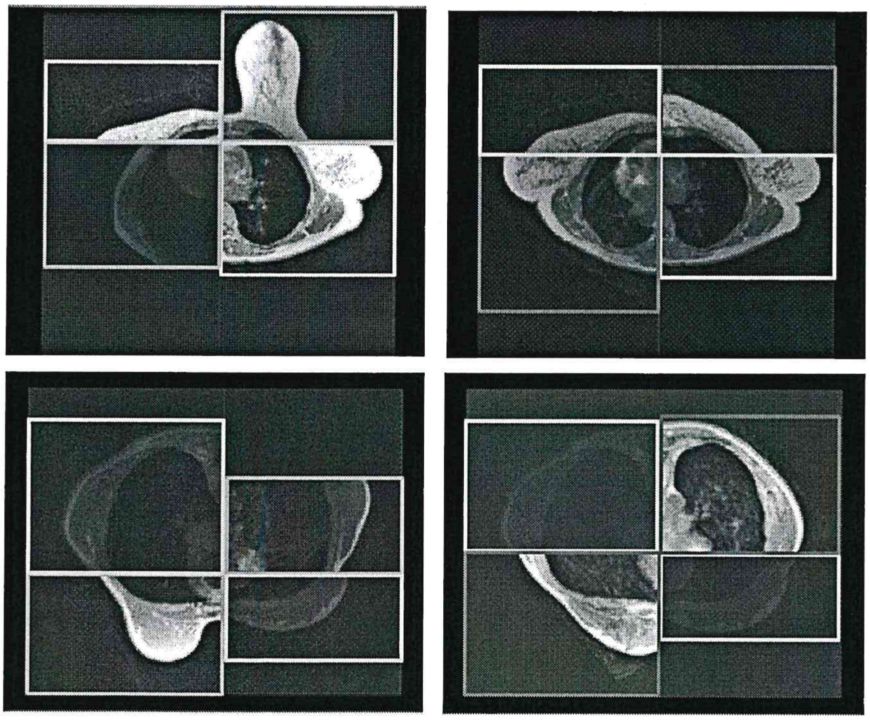

Figure 3.3: Registered MRI images: first line- subject 1; second line- subject 2; first column - prone configuration versus supine; second column - supine tilted versus supine

in that configuration

In a multi-gravity loading finite element~~s~~ simulation, the gravity force is applied to the whole model as a body force. The gravity fore orientation can be broken down into three components of the Cartesian coordinate system labeled X, Y, and Z directions. The supine configuration was chosen as a reference state, therefore the gravity loading direction was set to be oriented on the inverse direction of the ~~Z~~ Y axis (posterio-anterior direction): $\gamma_s = (0, -1, 0)$. The gravity loading direction for the two other positions are given by the rigid transformation computed by images registration: $\gamma_p = (0.037, 0.985, -0.165)$ direction vector for gravity in prone position and $\gamma_{st} = (-0.744, -0.667, 0.023)$ direction vector for supine tilted position~~.~~ for ~~the~~ volunteer [illegible].

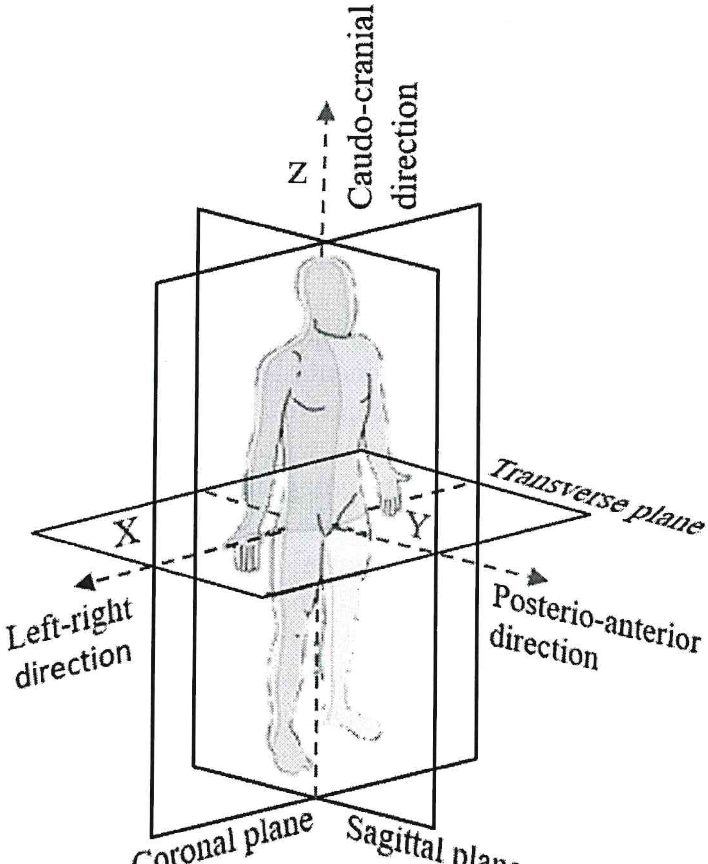

Figure 3.4: Anatomical planes and nominal Cartesian axis directions.

3.2.4 Patient-specific 3D geometry

The breast patient-specific geometry was created based on the MR images of the second ~~subject~~. Following image segmentation (Figure 3.5.b), the outer shape of labeled regions
volunteer

Des idées sur les erreurs entre les NURBS generées et les vraies surfaces reconstruites à partir de l'IRM ?

are subsequently discretized by 2D triangular elements. We used the semi-automatic Skin Surface module proposed by SpaceClaim Direct Modeler to convert the mesh surfaces to non-uniform rational basis spline (NURBS) surfaces. The NURBS are averaging curves between points, therefore they are smoother and easier to use in mechanical applications. The resulting two surfaces represent the 3D geometries of the breast and the thoracic cage with muscle (Figure 3.5.c).

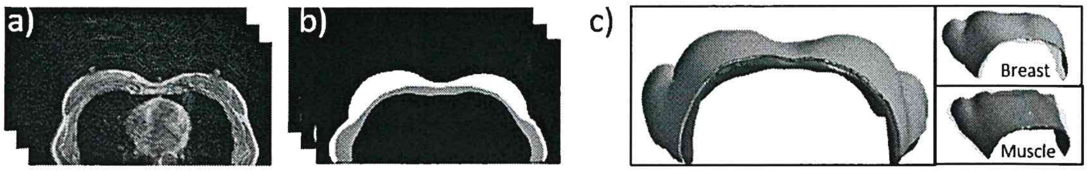

Figure 3.5: 3D geometries generation. a) MR images; b) segmeted image; c) corresponding 3D geometries

3.3 Finite Elements Mesh

such meshes

After computing the NURBS surfaces, the internal spatial information needs to be encoded using a volumetric mesh. The optimal elements type or mesh density in the simulation of FE models is still an open ~~problem~~ question and topic of debate. The use of hexahedral elements is usually assumed to result~~s~~ in a more accurate solution, especially when expecting high strain/stress gradients. However, in the literature, because of ~~the~~ their large computational time, ~~they~~ are used mostly with a reduced number of elements (Ruiter et al., 2006; Gamage et al., 2012). Tetrahedral elements are widely used due to their geometrical flexibility and because they provide a good trade-off between ~~the~~ computation time and displacement accuracy (Han et al., 2014; Palomar et al., 2008; Griesenauer et al., 2017). to estimate the constitutive parameters. Therefore, to reduce

In our case, an iterative optimization process is being considered, ~~thus to reduce~~ the computation time, only linear tetrahedral elements are used. The first order elements are known to bear volumetric locking problems when used to model large strain for quasi-incompressible materials, (Fung et al., 2017). When volumetric locking occurs, the displacements calculated by the finite element method are orders of magnitude smaller than they should be. It has been shown that a linear element with a mixed U-P formulation can avoid these problems (Rohan et al., 2014). therefore, in our work, the geometries are meshed using the solid element solid285 (ANSYS Mechanical) which provides a mixed U-P formulation option.

On the other hand, the mesh density has also an impact on model accuracy, a finer mesh result~~s~~ing ~~in~~ a more accurate and stable solution, but also increas~~e~~ing the computational time. ~~So far~~ To our knowledge, no ~~experimental~~ studies have determined the optimal resolution of the volumetric mesh for simulating ~~of~~ breast tissues deformations. To determinate the appropriate mesh size, a mesh convergence study was performed. The details can be found in annex .... According to these results the optimal elements sizes range between 7 and 10mm. The that was chosen for volunteer 2 thus

~~chosen~~ mesh consists in 18453 elements with 9625 elements assigned to the pectoral muscle and the thoracic cage and 8828 elements assigned to breast tissues (Figure 3.7). à mettre en 3.6

The mesh quality is measured using three criteria: element skewness, aspect ratio and maximal corner angle. The Figure 3.6 (3.7) shows the ranges of values for ~~different elements~~ these shape parameters. The element's aspect ratio and maximal corner angle range between the nominal limits defining a good mesh quality (Section 2.3). There is a small number of elements with a skewness lager than the maximal theoretical quality limit (0.75) , however there are no degenerated elements (skewness = 1).

Figure 3.6: Finite elements mesh quality.

The breast skin layer is added a posteriori as a $2mm$ thick single layer of shell elements (1980 elements). Shell elements and the underlying solid elements are sharing the same nodes (Figure 3.7).

A mettre avant la figure 3.6, non?

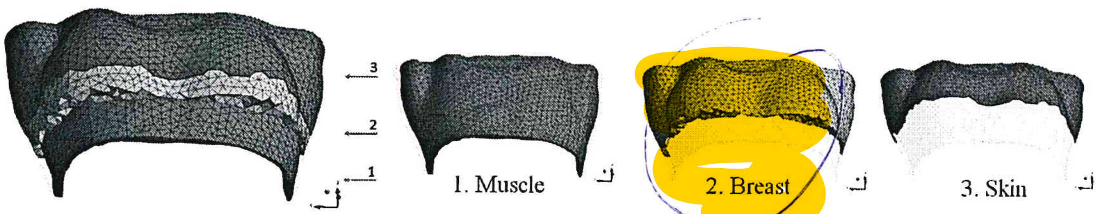

Figure 3.7: Finite elements mesh components. The tissues components are cropped for visualization purposes.

Tu n'as expliqué nulle part pourquoi tu fais l'hypothèse de ne pas distinguer les tissus glandulaires et les tissus gras. Il faudrait le dire, non?

3.4 Breast reference configuration

citer une référence ("stress free" configuration)

To estimate the reference configuration of the breast, an adapted prediction-correction iterative approach was implemented. Prone and supine image data sets are used to compute the stress-free geometry. The overall iterative process is presented in Figure 3.8. The first estimate of stress-free breast configuration is ~~obtained by~~ inverse gravity on the supine ~~geometry~~ position. Then, at each iteration, the estimated stress-free configuration is used to simulate breast deformation due to gravity in a prone position. The differences between result of this simulation and the real shape of the breast in prone position is quantified by computing the Euclidian distances D_i between the *active nodes* defined at the breast external surface. ~~This~~ These distances ~~is~~ are then used in the next iteration of our process to simulate ~~an~~

computed by the model by applying on

imposed displacements (Dirichlet condition) to the active nodes i in the stress-free condition. To limit any mesh distortion, the displacements ~~is~~ are only partially imposed using a multiplicative regularization factor ($\alpha < 1$). The process repeats as long as the new transformation improves the similarity between the ~~two~~ geometries by more than $1mm$ on average. The similarity between the estimated and measured prone breast configurations is given by the mean Euclidean distance over the active nodes.

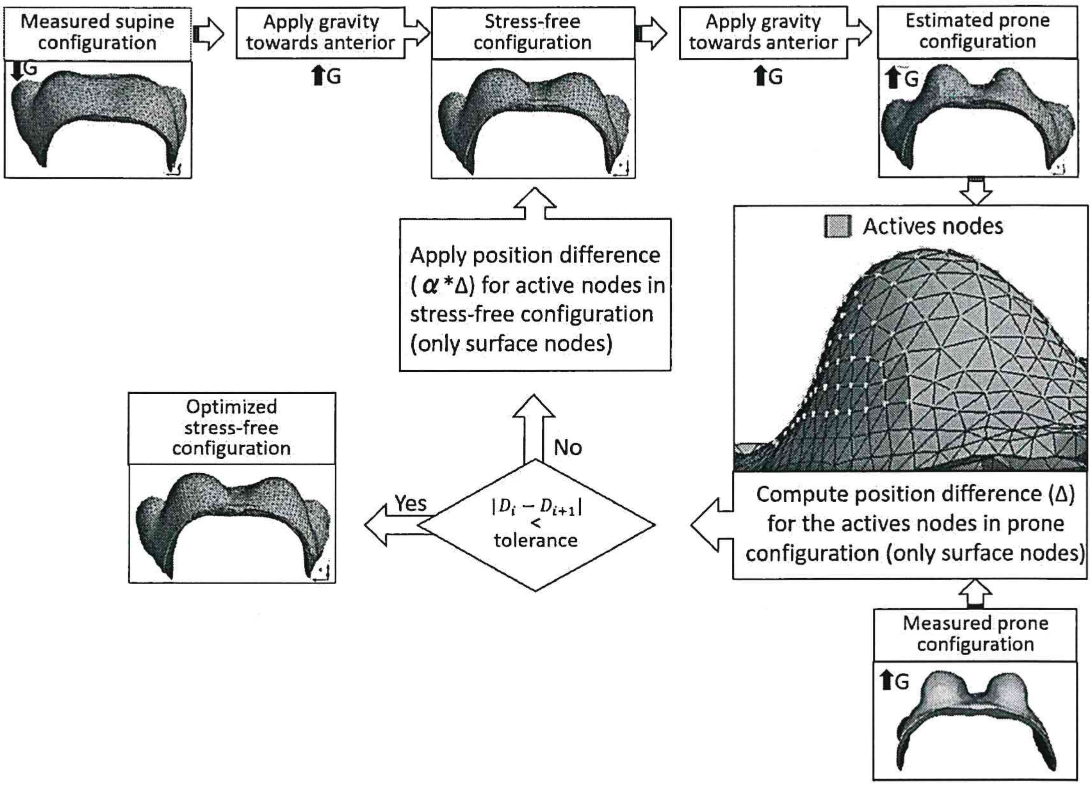

Figure 3.8: Fixed point type iterative algorithm for stress-free geometry approximation. D_i - mean node to node distance over the active nodes at iteration i, G - gravity force

To compute the position difference D_i of the nodes i between the estimated and the measured breast configurations, the positions of the active surface nodes on prone configuration have to be known. Thus, a non-rigid additional mesh registration step is performed at each iteration: the active nodes are morphed into prone configuration using the elastic deformation method proposed by Bucki et al. (2010). The method estimates a C1-diffeomorphic, non-folding and one-to-one transformation to register a source point cloud onto a target data set D, which can either be a point cloud or a surface mesh. The input source points set is initially embedded in a deformable virtual hexahedral elastic grid. Then an iterative registration technique is performed by successive elementary grid deformations and at different grid refinement levels.

3.5 Boundary conditions

Breast deformations can be modeled by solving the motion equations using two different types of boundary conditions, regarding either displacements (Dirichlet conditions) or forces (Neumann conditions).

assumed to be attached to the rib cage

First, to provide a rigid support for the muscle mesh component, zero displacement conditions are imposed to its posterior face (figure 3.9). Next, the interface between the breast mesh and muscle mesh is modeled using contact mechanics. The muscle is stiffer than the adipose tissues, thus it's anterior face represents the target surface and the posterior breast face represents the contact surface. (see § 2.4 for a reminder of these target and source surfaces)

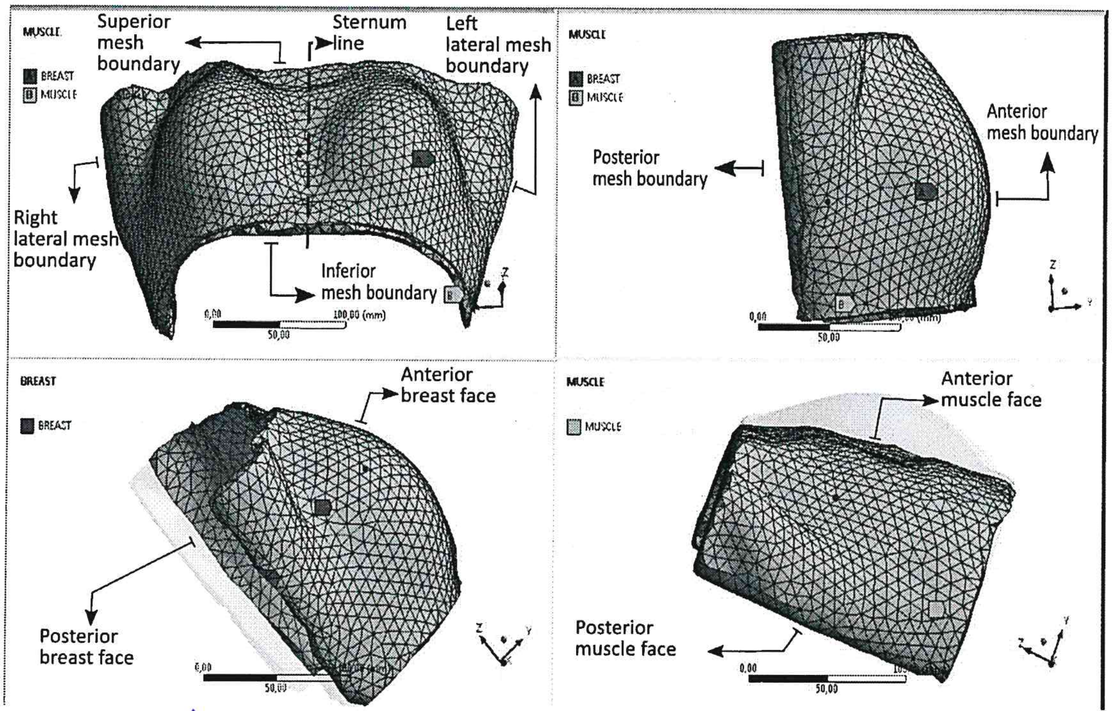

Figure 3.9: Finite element~~s~~ mesh boundaries

requires to take into account

shown

Previous works have ~~proved~~ that ~~to~~ modeling breast deformations from prone to supine configurations breast tissues' sliding over the chest wall ~~have to be considered~~. (Carter et al., 2012; Han et al., 2014). Moreover, anatomical books (Mugea and Shiffman, 2014; Clemente, 2011)~~s~~ describe that the breast soft tissues are firmly attached to the deep fascia via suspensory ligaments but can move freely over the pectoralis muscle. Therefore, the juncture surface is modeled as a no-separation contact with a frictional behavior proposed by the ANSYS Contact Technologies (see Section 2.4.2). The ~~P~~penalty algorithm is used with a meticulous control of contact normal and opening stiffness parameters. Stiffness parameters don't have a physical meaning and have to be identified by *trial and error* methods. since these parameters ~~Because they~~ are extremely sensitive to the underlying elements stiffness and to the local deformation direction, new values have to be identified for each new simulation case.

Il y a trop de glissement si μ_f est grand ?

To study the impact of the friction~~al~~ coefficient μ_f ~~parameter~~ on tissues sliding, several simulations have been performed at different values of μ_f. We found that, with the Coulomb~~s~~ friction law, even for a high value of μ_f, the tissues sliding is overestimated. When simulating prone breast configuration from the supine one, the sliding overestimation results also in an unconvergent solution due to element distortion. At the contact surface, because of excessive sliding, the tissue~~s~~ accumulation in the region of the sternum line results in a sinuous surface (Figure 3.10) ; the finite element~~s~~ most undergo important distortion~~s~~ and the solution is compromised. Therefore, different strategies based on anatomical breast structures were investigated to limit the amount of sliding and to overcome solution instabilities (Annex 2). However, it seems that a small amount of friction improves the solution convergence capabilities (~~refer~~ see ansys manual); ~~thus~~ therefore the friction coefficient is kept to $\mu_f = 0.1$.

donner une ref biblio

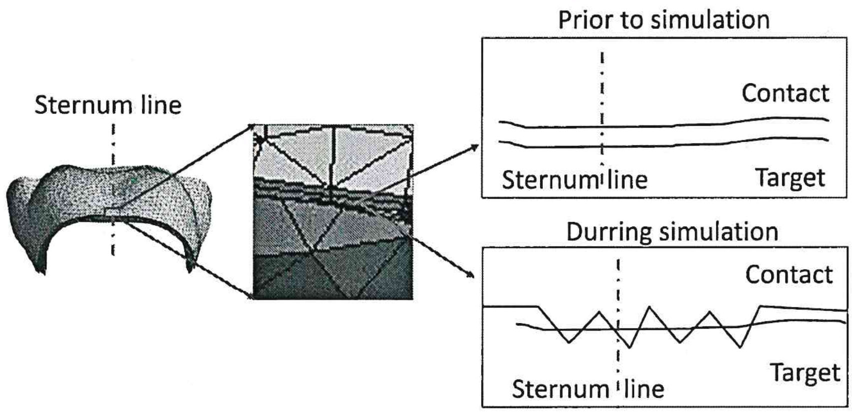

Figure 3.10: Tissues acumulation on the sternum line with excessive sliding

The strategy chosen to control the amount of tissues sliding relies on ligamentous breast structures described on Section 1.2.3. As concerns ~~From~~ breast support matrix only, the largest structures are modeled, i.e. fascias and suspensory ligaments. The Superficial layer of superficial fascia is integrated in the skin layer, assuming a higher material stiffness. In addition, a new layer of 0.1mm thick shell elements is added at the juncture surface between muscle and breast tissue to model the deep layer of the superficial fascia. Shell elements and the underlying breast elements are sharing the same nodes. Since the deep fascia and muscle tissue~~s~~ are supposed to present similar elastic properties, the deep fascia is not explicitly modeled. In addition, ~~Two~~ two ligamentous structures (inframammary ligament and deep medial ligament) are modeled using Ansys link type elements connecting breast posterior surface nodes to anterior muscle surface nodes (Figure 3.11).

Several additional Dirichlet conditions are set on the mesh boundaries: the superior and inferior ends of the deep fascia layer are constrained in Z direction; the superior and inferior ends of the skin layer are constrained in Y direction. For left and right lateral breast boundaries (Figure 3.9), Dirichlet conditions are too strong and preclude breast tissue to slide laterally. Therefore, in these regions new ligamentous structures are included with a cable-like